

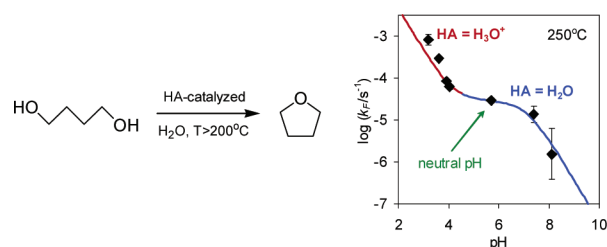
## Kinetics and Mechanism of Tetrahydrofuran Synthesis via 1,4-Butanediol Dehydration in High-Temperature Water

Shawn E. Hunter, Carolyn E. Ehrenberger, and Phillip E. Savage\*

Department of Chemical Engineering, The University of Michigan, Ann Arbor, Michigan 48109–2136

E-mail: psavage@umich.edu.

Received May 17, 2006



We conducted an experimental investigation into the kinetics and mechanism of tetrahydrofuran synthesis from 1,4-butanediol via dehydration in high-temperature liquid water (HTW) without added catalyst at 200–350 °C. The reaction was reversible, with tetrahydrofuran being produced at an equilibrium yield of 84% (at 200 °C) to 94% (at 350 °C). The addition of CO<sub>2</sub> to the reaction mixture increased the reaction rate by a factor of 1.9–2.9, because of the increase in acidity resulting from the formation and dissociation of carbonic acid. This increase was much less than that expected (factor of 37–60) from a previously suggested acid-catalyzed mechanism. This disagreement prompted experiments with added acid (HCl) and base (NaOH) to investigate the influence of pH on the reaction rate. These experiments revealed three distinct regions of pH dependence. At high and low pH, the dehydration rate increased with increasing acidity. At near-neutral pH, however, the rate was essentially insensitive to changes in pH. This behavior is consistent with a mechanism where H<sub>2</sub>O, in addition to H<sup>+</sup>, serves as a proton donor. This work indicates that the relatively high native concentration of H<sup>+</sup> (large K<sub>w</sub>), which has commonly been thought to lead to the occurrence of acid-catalyzed reactions in HTW without added catalyst, does not explain the dehydration of 1,4-butanediol in HTW without catalyst. Rather, H<sub>2</sub>O serves directly as the proton donor for the reaction.

### Introduction

Tetrahydrofuran (THF) is a cyclic ether used in a wide range of industrial processes. Almost 400,000 metric tons of THF were produced in 2003.<sup>1</sup> Roughly <sup>4</sup>/<sub>5</sub> of THF produced is polymerized to form polytetramethylene glycol (PTMEG), which is used to produce elastic (Spandex) fibers, polyurethane elastomers, and copolyester-ether elastomers.<sup>1,2</sup> The remaining <sup>1</sup>/<sub>5</sub> of THF is used as a solvent in the production of poly(vinyl chloride) (PVC) cements and coatings, pharmaceuticals, magnetic tapes and films, and in Grignard reactions.<sup>1,2</sup> THF may also be used as the starting material for producing succinic acid, adipic acid, and  $\gamma$ -valerolactone.<sup>2</sup>

THF can be obtained via several synthetic routes, with acetylene and formaldehyde (Repe process), propylene oxide, *n*-butane, and furfural each serving as different feedstocks.<sup>1,2</sup> The most commonly applied commercial route is the Repe process,<sup>1,2</sup> wherein THF is obtained directly from the acid-catalyzed dehydration of 1,4-butanediol (BD). BD dehydration is also a key reaction in the propylene oxide process, which is also applied commercially.<sup>1</sup> In other processes<sup>1–3</sup> a mixture of BD and THF is formed in the final step, and hence BD dehydration can be used to increase overall selectivity to THF. BD dehydration is thus a significant reaction for many industrial processes that produce THF.

In the Repe and propylene oxide processes, BD dehydration is achieved in the presence of an acid catalyst at temperatures above 100 °C and near atmospheric pressure.<sup>2</sup> Effective catalytic

\* Fax: +1 734 763 0459. Tel: +1 734 764 3386.

(1) Ring, K. L.; Kalin, T.; Yokose, K. In *Chemical Economics Handbook*; Stanford Research Institute: Menlo Park, CA, 2004; p 695.3000C–F.

(2) Muller, H. In *Ullmann's Encyclopedia of Industrial Chemistry*, 6th ed.; Wiley-VCH: Weinheim, Germany, 2003; Vol. 35, p 671.

(3) Bertola, A. U.S. Patent 6,248,906, 2001.

agents include strong mineral acids,<sup>4</sup> heteropolyacids,<sup>5,6</sup> zeolites,<sup>7</sup> sulfonic acids,<sup>8,9</sup> and dimethyl sulfoxide (DMSO).<sup>10</sup> Strong mineral acids, aluminum silicates, and ion-exchange resins are the preferred commercial catalysts,<sup>1,2,9</sup> and THF is typically produced at 95% yield.<sup>1</sup>

The acid catalysts in the current processes create undesired environmental and economic burdens. For example, mineral acids are corrosive and often necessitate the use of corrosion-resistant materials. Additionally, these acids are typically neutralized after the reaction, which consumes both the catalyst and the neutralizing agent and generates waste salt. Solid acids avoid the corrosion and neutralization issues of mineral acids, but often require frequent regeneration or replacement owing to catalyst deactivation.

A cleaner, more environmentally benign approach for synthesizing THF from BD may be the use of high-temperature liquid water (HTW) as the reaction medium. Liquid water at elevated temperatures ( $T > 200$  °C) has received much recent attention as an alternative reaction medium for organic synthesis.<sup>11–14</sup> Under these conditions, water exhibits increased solubility for small organic compounds typically thought of as being insoluble in water.<sup>15</sup> In addition, HTW can facilitate the occurrence of some classically acid- and base-catalyzed reactions, even in the absence of any added catalyst.<sup>11,12,16</sup> This ability has often been attributed<sup>17–24</sup> to the relatively large value of the ion product  $K_W$  in HTW, and associated high native concentrations of  $H^+$  and  $OH^-$  ions, coupled with the elevated temperature of HTW. Further, conducting the reaction in HTW enables the possibility of accelerating the rate through the addition of  $CO_2$ , an environmentally benign additive.<sup>12,25</sup> Enhancement of BD dehydration via added  $CO_2$  could provide competitive reaction rates for a HTW-based process, without the environmental concerns associated with mineral acid.

- (4) Hudson, B. G.; Barker, R. *J. Org. Chem.* **1967**, *32*, 3650–3658.
- (5) Török, B.; Bucsi, I.; Bereszászi, T.; Kapocsi, I.; Molnár, A. *J. Mol. Catal. A: Chem.* **1996**, *107*, 305–311.
- (6) Baba, T.; Ono, Y. *J. Mol. Catal.* **1986**, *37*, 317–326.
- (7) Rao, Y. V. S.; Kulkarni, S. J.; Subrahmanyam, M.; Rao, A. V. R. *J. Org. Chem.* **1994**, *59*, 3998–4000.
- (8) Bucsi, I.; Molnár, A.; Bartók, M. *Tetrahedron* **1995**, *51*, 3319–3326.
- (9) Limbeck, U.; Altwicker, C.; Kunz, U.; Hoffmann, U. *Chem. Eng. Sci.* **2001**, *56*, 2171–2178.
- (10) Molnár, A.; Bartók, M. *Helv. Chim. Acta* **1981**, *64*, 389–398.
- (11) Savage, P. E. *Chem. Rev.* **1999**, *99*, 603–621.
- (12) Hunter, S. E.; Savage, P. E. *Chem. Eng. Sci.* **2004**, *59*, 4903–4909.
- (13) Broll, D.; Kaul, C.; Kramer, A.; Krammer, P.; Richter, T.; Jung, M.; Vogel, H.; Zehner, P. *Angew. Chem., Int. Ed.* **1999**, *38*, 2998–3014.
- (14) Akiya, N.; Savage, P. E. *Chem. Rev.* **2002**, *102*, 2725–2750.
- (15) Chandler, K.; Eason, B.; Liotta, C. L.; Eckert, C. A. *Ind. Eng. Chem. Res.* **1998**, *37*, 3515–3518.
- (16) Kuhlmann, B.; Arnett, E. M.; Siskin, M. *J. Org. Chem.* **1994**, *59*, 3098–3101.
- (17) Chamblee, T. S.; Weikel, R. R.; Nolen, S. A.; Liotta, C. L.; Eckert, C. A. *Green Chem.* **2004**, *6*, 382–386.
- (18) Chandler, K.; Deng, F. H.; Dillow, A. K.; Liotta, C. L.; Eckert, C. A. *Ind. Eng. Chem. Res.* **1997**, *36*, 5175–5179.
- (19) Chandler, K.; Liotta, C. L.; Eckert, C. A.; Schiraldi, D. *AIChE J.* **1998**, *44*, 2080–2087.
- (20) Glaser, R.; Brown, J. S.; Nolen, S. A.; Liotta, C. L.; Eckert, C. A. *Abstr. Pap. Am. Chem. Soc.* **1999**, *217*, U820–U820.
- (21) Lesutis, H. P.; Glaser, R.; Liotta, C. L.; Eckert, C. A. *Chem. Commun.* **1999**, 2063–2064.
- (22) Nolen, S. A.; Liotta, C. L.; Eckert, C. A.; Glaser, R. *Green Chem.* **2003**, *5*, 663–669.
- (23) Patrick, H. R.; Griffith, K.; Liotta, C. L.; Eckert, C. A.; Glaser, R. *Ind. Eng. Chem. Res.* **2001**, *40*, 6063–6067.
- (24) Sato, K.; Kishimoto, T.; Morimoto, M.; Saimoto, H.; Shigemasa, Y. *Tetrahedron Lett.* **2003**, *44*, 8623–8625.
- (25) Hunter, S. E.; Savage, P. E. *Ind. Eng. Chem. Res.* **2003**, *42*, 290–294.

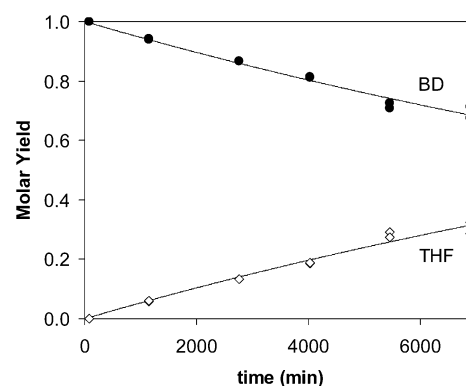


**FIGURE 1.** Molar yield of 1,4-butanediol and THF in HTW at 200 °C.  $C_{BD,0} = 0.3$  mol/kg. Curves represent the fit of eqs 3 and 4 to the data.

BD dehydration in HTW has been investigated previously. Richter and Vogel<sup>26</sup> conducted BD dehydration experiments at 300–400 °C and residence times under three minutes using a flow reactor. They found that THF could be produced in high (near 100%) selectivity from BD in HTW and supercritical water (SCW,  $T > 374$  °C) without catalyst. They reported that the reaction was irreversible, but did not investigate conversions greater than about 60%. Nagai et al.<sup>27</sup> examined the dehydration of BD using glass tube batch reactors, in both high-temperature liquid  $D_2O$  at 150–365 °C and supercritical  $D_2O$  at 385–400 °C and with added mineral acid. On the basis of a kinetic analysis, they concluded that a “water-induced” reaction was significant for BD dehydration in neutral HTW. This conclusion differed from that of Richter and Vogel, who proposed catalysis by  $H^+$  as the dominant mechanism.

To further investigate the applicability of HTW as a reaction medium for THF synthesis, and especially to elucidate the mechanism of BD dehydration in HTW, we conducted a detailed study of THF synthesis via BD dehydration in HTW. Here, we present the results of THF synthesis experiments at 200–350 °C for batch holding times of up to 115 h. We also examine the potential for added  $CO_2$  to accelerate the dehydration reaction. We then explore the kinetics and mechanism of BD dehydration in HTW, over a wide range of pH, and provide evidence confirming that an  $H^+$ -catalyzed mechanism for BD dehydration is not the dominant mechanism in near-neutral HTW. Rather, we demonstrate that  $H_2O$  serves as the proton donor and catalyst for BD dehydration in HTW without added catalyst.

## Results and Discussion

This section provides information about the influence of temperature, added  $CO_2$ , and pH on the reaction kinetics. We then use this information to draw inferences about the mechanism governing THF synthesis in HTW.

**Kinetics.** Figures 1, 2, 3, and 4 show yield versus time profiles for experiments at 200, 250, 300, and 350 °C, respectively. Under the conditions examined, BD dehydrates in HTW without added catalyst to selectively yield THF. Figures 3 and 4 demonstrate that the reaction is reversible, with the

(26) Richter, T.; Vogel, H. *Chem. Eng. Technol.* **2001**, *24*, 340–343.

(27) Nagai, Y.; Matubayasi, N.; Nakahara, M. *Bull. Chem. Soc. Jpn.* **2004**, *77*, 691–697.

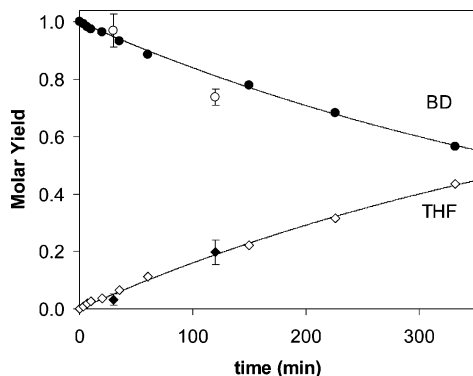


**FIGURE 2.** Molar yield of 1,4-butanediol and THF in HTW at 250 °C.  $C_{BD,0} = 0.3$  mol/kg. Curves represent the fit of eqs 3 and 4 to the autoclave data. Tubing bomb data are shown as open circles (BD yield) and filled diamonds (THF yield).

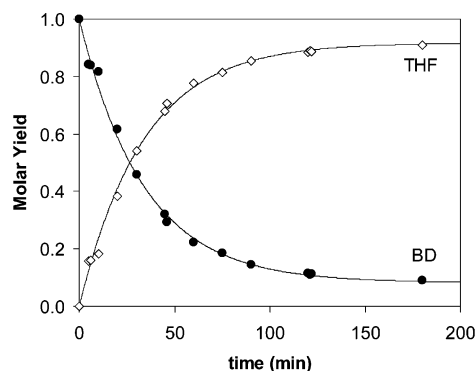


**FIGURE 3.** Molar yield of 1,4-butanediol and THF in HTW at 300 °C.  $C_{BD,0} = 0.4$  mol/kg. Curves represent the fit of eqs 3 and 4 to the data.

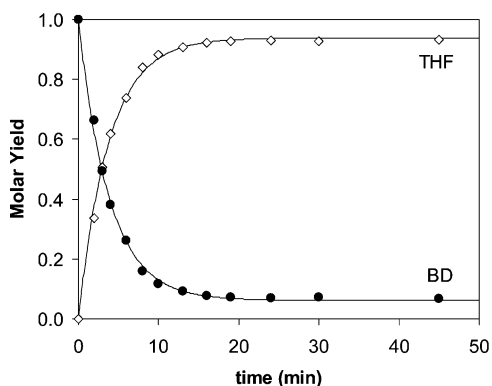


**FIGURE 4.** Molar yield of 1,4-butanediol and THF in HTW at 350 °C.  $C_{BD,0} = 0.5$  mol/kg. Curves represent the fit of eqs 3 and 4 to the data.

equilibrium yield of THF being greater than 90% at these temperatures.

We performed a kinetic analysis to obtain forward ( $k_F$ ) and reverse ( $k_R$ ) rate constants for the conversion of BD to THF. For a reversible reaction with pseudo-first-order kinetics<sup>26</sup> in a constant-volume batch reactor, the following differential equations apply for BD and THF:

$$\frac{d[\text{BD}]}{dt} = r_{\text{BD}} = -k_F[\text{BD}] + k_R[\text{THF}] \quad (1)$$

$$\frac{d[\text{THF}]}{dt} = r_{\text{THF}} = k_F[\text{BD}] - k_R[\text{THF}] \quad (2)$$

These equations can be recast in terms of molar yield  $Y_i = C_i/C_{BD,0}$  as

$$\frac{dY_{\text{BD}}}{dt} = -k_F Y_{\text{BD}} + k_R Y_{\text{THF}} \quad (3)$$

$$\frac{dY_{\text{THF}}}{dt} = k_F Y_{\text{BD}} - k_R Y_{\text{THF}} \quad (4)$$

We fit the experimental yield versus time data in Figures 1–4 to eqs 3 and 4 to estimate  $k_F$  and  $k_R$  at each temperature. We employed the modeling software Scientist<sup>28</sup> to perform an unweighted, nonlinear least-squares analysis. Table 1 lists the estimated values of  $k_F$  and  $k_R$  at each temperature. Fitting the data at 200 °C led to a value of zero for  $k_R$ , because of the relatively low conversion at this temperature. Thus, at 200 °C we report only  $k_F$ . The agreement between the model and experimental data is shown at each temperature by the curves in Figures 1–4. These figures demonstrate that the model provides a good description of the data over the entire experimental temperature range of 200–350 °C.

Figure 2 displays the BD and THF yields obtained in preliminary experiments at 250 °C with tubing bomb reactors. The agreement of these data with the autoclave reactor data demonstrates that consistent kinetics were obtained in both types of reactors.

Hudson and Barker<sup>4</sup> provide  $k_F$  in 2 M HCl at 99 °C as  $5.1 \times 10^{-5} \text{ s}^{-1}$ . Table 1 shows that  $k_F$  is on the same order of magnitude in HTW at 250 °C, and is 1 and 2 orders of magnitude greater at 300 °C and 350 °C, respectively. Thus, the rate of BD dehydration in HTW without added catalyst is comparable and even superior to that in strong acid solutions at lower temperature.

The concentration of  $\text{H}_2\text{O}$ , which is a product of the reaction, is lumped into the reverse rate constant  $k_R$ . To remove the effect of the temperature-dependent water concentration from the estimated reverse rate constant, we also obtained estimates for the second order reverse rate constant  $k'_R$ , defined as  $k'_R = k_R/(\text{H}_2\text{O})$ . Table 1 displays the estimated values of  $k'_R$ .

Table 1 also provides the Arrhenius activation energy and preexponential factor for each rate constant. Hudson and Barker<sup>4</sup> report the activation energy for the dehydration of BD at 90–123 °C in 2 M HCl to be 31 kcal mol<sup>-1</sup>. Nagai et al.<sup>27</sup> report the activation energy for the dehydration in HTW ( $\text{D}_2\text{O}$ ) without catalyst to be 29 kcal mol<sup>-1</sup>. Our estimate of  $32.8 \pm 2.0$  kcal mol<sup>-1</sup> agrees well with these previous values.

Having obtained rate constant estimates for the conversion of BD to THF, we next estimated the equilibrium constant and equilibrium yield of THF at each experimental temperature. The equilibrium yield  $Y_{\text{THF,EQ}}$  can be obtained by setting eq 3 equal to zero, noting that  $Y_{\text{BD}} = 1 - Y_{\text{THF}}$ , and combining the two equations to solve for  $Y_{\text{THF}}$ :

$$Y_{\text{THF,EQ}} = \frac{K}{1 + K} \quad (5)$$

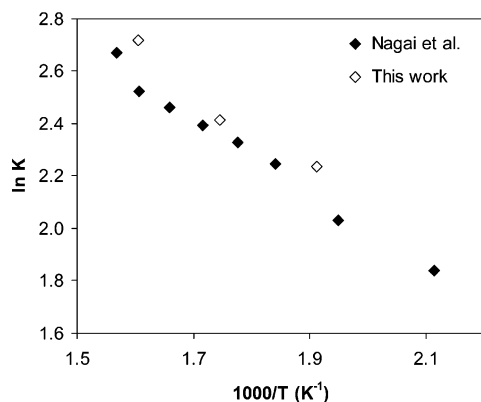
where the equilibrium constant  $K$  is defined as  $K = k_F/k_R = Y_{\text{THF,EQ}}/Y_{\text{BD}}$ . The equilibrium constants and equilibrium yields of

(28) Scientist, version 2.01; MicroMath, Inc.: Salt Lake City, UT, 1995.

**TABLE 1.** Parameter Estimates for the Forward and Reverse Rate Constants for 1,4-Butanediol Dehydration in HTW<sup>a</sup>

	pH	$k_F \times 10^5$ (s <sup>-1</sup> )	$k_R \times 10^5$ (s <sup>-1</sup> )	$k'_R \times 10^7$ (L mol <sup>-1</sup> s <sup>-1</sup> )	K	$K'$ (mol L <sup>-1</sup> )	$Y_{\text{THF-EQ}}$
$T = 200$ (°C)	5.7	$0.091 \pm 0.005$					0.84 <sup>b</sup>
$T = 250$ (°C)	5.7	$2.9 \pm 0.3$	$0.31 \pm 1.07$	$0.71 \pm 2.5$	9.4	415	0.90
$T = 300$ (°C)	5.9	$45 \pm 3$	$4.0 \pm 1.5$	$10 \pm 4$	11	441	0.92
$T = 350$ (°C)	6.4	$405 \pm 22$	$27 \pm 8$	$84 \pm 24$	15	482	0.94
$\log A$ (s <sup>-1</sup> )		$9.1 \pm 0.8$	$6.6 \pm 5.2$	$5.8 \pm 2.8$			
$E_a$ (kcal mol <sup>-1</sup> )		$32.8 \pm 2.0$	$28.8 \pm 13.5$	$31.0 \pm 7.4$			

<sup>a</sup> Uncertainties represent the 95% confidence interval. <sup>b</sup> The equilibrium THF molar yield at 200 °C was calculated based on an extrapolated value of  $k_R$ , which was obtained using the Arrhenius equation.

**FIGURE 5.** Equilibrium constant for BD dehydration in HTW as a function of temperature.

THF appear in Table 1. The equilibrium THF yield is 84% at 200 °C and increases to 94% at 350 °C, indicating that the reaction is endothermic.

Figure 5 shows a comparison of the equilibrium constants estimated from the data in Figures 1–4 with those reported by Nagai et al.<sup>27</sup> for this reaction in HTW. The figure shows good agreement between the two sets of data, with the previous data being slightly lower than the new data reported here. One explanation for this slight difference may be the experimental technique. In the present work, liquid-phase samples were acquired from a 440 mL reactor using a dip tube. Nagai et al., however, performed experiments using 1.0 mL quartz tubes. The entire contents of those tubes were recovered for analysis, and the tubes were loaded with a specified amount of water at room temperature (for example, 0.5 mL at  $T < 350$  °C). At the water loadings specified in Nagai et al., a considerable amount of vapor space would have occupied the 1.0 mL reactor at the reaction temperature. For example, at 250 °C, the vapor phase would have occupied roughly 40% of the reactor volume, based on the density of saturated water.<sup>29</sup> In the autoclave reactor used in our work, a much smaller portion of the reactor volume (~5%) was available for the coexisting vapor phase. Thus, there may have been more partitioning of organics into the vapor phase during the Nagai et al. experiments, leading to a lower observed BD conversion based on the total amount of BD loaded.

To estimate the heat of reaction ( $\Delta H_{\text{rxn}}$ ) for BD dehydration, which has not been reported previously, we applied the van't Hoff equation. Assuming the heat of reaction to be independent of temperature over the range investigated, one obtains

$$\ln K' = \left( \frac{-\Delta H_{\text{rxn}}}{R} \right) \frac{1}{T} + b \quad (6)$$

where  $K' = k_F/k'_R = (\text{THF})(\text{H}_2\text{O})/(\text{BD})$  and  $b$  is a constant. We utilized  $K'$ , rather than  $K$ , in our estimation of  $\Delta H_{\text{rxn}}$  to

again decouple water concentration effects from the estimated parameter. By performing linear regression of  $\ln K'$  vs  $1/T$  data at 250–350 °C, we estimated  $\Delta H_{\text{rxn}}$  to be 1.0 kcal mol<sup>-1</sup> with a standard error of 0.2 kcal mol<sup>-1</sup>.

To compare this experimental value for  $\Delta H_{\text{rxn}}$  in HTW with that at lower temperatures, we calculated the standard heat of reaction  $\Delta H_{\text{rxn}}^0$  for 1,4-butanediol dehydration in the liquid phase as

$$\Delta H_{\text{rxn}}^0 = \Delta H_f^0(\text{THF}, l) + \Delta H_f^0(\text{H}_2\text{O}, l) - \Delta H_f^0(\text{BD}, l) \quad (7)$$

where  $\Delta H_f^0(i, l)$  is the standard heat of formation of species  $i$  in the liquid phase. We obtained  $\Delta H_f^0(\text{BD}, l)$  and  $\Delta H_f^0(\text{H}_2\text{O}, l)$  from Knauth and Sabbah<sup>30</sup> and Chase,<sup>31</sup> respectively.  $\Delta H_f^0(\text{THF}, l)$  has not been reported previously, so we estimated its value from the standard heat of combustion  $\Delta H_c^0(\text{THF}, l)$  of THF<sup>32</sup> using

$$\Delta H_f^0(\text{THF}, l) = -\Delta H_c^0(\text{THF}, l) + 4\Delta H_f^0(\text{H}_2\text{O}, l) + 4\Delta H_f^0(\text{CO}_2, g) \quad (8)$$

where  $\Delta H_f^0(\text{CO}_2, g)$  is the standard heat of formation of gas-phase  $\text{CO}_2$ , also obtained from Chase.<sup>31</sup> Using eq 7, we calculated the standard heat of reaction for BD dehydration in the liquid phase to be 2 kcal mol<sup>-1</sup>. This value is close to the experimental value of 1.0 kcal mol<sup>-1</sup> determined for the reaction at higher temperatures.

**Effect of Added CO<sub>2</sub>.** We performed 1,4-butanediol dehydration experiments in HTW with added CO<sub>2</sub> at 250 and 300 °C. Figure 6 shows that at both temperatures, the reaction was accelerated by the addition of CO<sub>2</sub>. For example, at 250 °C and 60 min of reaction time, the experimental THF yield increased from 11% to 25% with the addition of CO<sub>2</sub>. At 300 °C, the THF yield in HTW at 20 min was 38%, but it increased to 59% at only 18 min with added CO<sub>2</sub>. Hence, CO<sub>2</sub> addition is effective for accelerating the synthesis of THF from 1,4-butanediol dehydration in HTW.

To quantify the effect of added CO<sub>2</sub> on the reaction, we estimated  $k_F$  and  $k_R$  using the data in Figure 6. Table 2 provides these rate constant estimates, obtained with Scientist using an unweighted least-squares regression. We next compared the experimentally observed increase in rate constant due to added CO<sub>2</sub> to that expected on the basis of the mechanism suggested previously by Richter and Vogel<sup>26</sup> for BD dehydration in HTW. Scheme 1 illustrates their acid-catalyzed mechanism. The reaction is initiated by protonation of an alcohol group by a

(29) Harvey, A. H. *NIST/ASME Steam Properties*, version 2.2; National Institute of Standards and Technology: Boulder, CO, 1996.

(30) Knauth, P.; Sabbah, R. *Struct. Chem.* **1990**, *1*, 43–46.

(31) Chase, M. W. *J. Phys. Chem. Ref. Data Monograph* **9** **1998**, 1–1951.

(32) Cox, J. D.; Pilcher, G. *Thermochemistry of Organic and Organometallic Compounds*; Academic Press: New York, 1970.

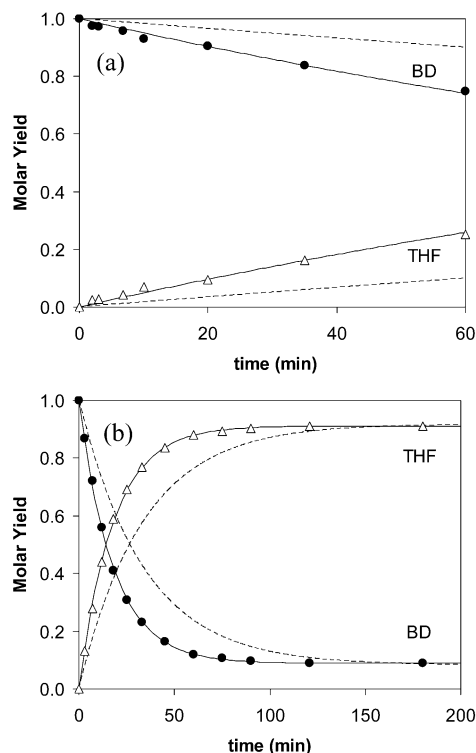
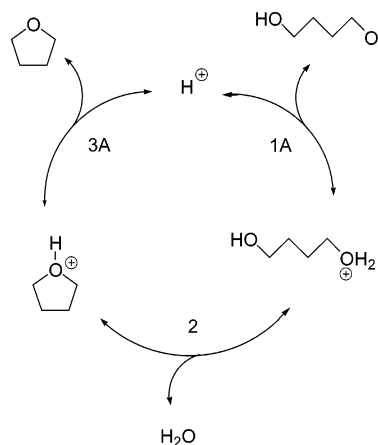


**FIGURE 6.** Molar yields of 1,4-butanediol and THF in HTW with added CO<sub>2</sub>. The dashed lines represent the molar yields of BD and THF in HTW without added CO<sub>2</sub>, calculated using eqs 3 and 4 and the parameters in Table 1: (a) 250 °C, C<sub>BD,0</sub> = 0.4 mol/kg, and the average reactor pressure was 152 bar; (b) 300 °C, C<sub>BD,0</sub> = 0.4 mol/kg, and the average reactor pressure was 183 bar.

**TABLE 2.** Comparison of Experimental and Expected Rate Increase Factor (RIF) for the CO<sub>2</sub>-Added BD Dehydration Experiments at 250 and 300 °C

T (°C)	P <sub>CO<sub>2</sub></sub> (bar)	estimated pH	k <sub>F</sub> × 10 <sup>5</sup> (s <sup>-1</sup> )	exptl RIF	expected RIF
250	112	3.9	8.5 ± 0.8	2.9	60
300	97	4.3	85 ± 2	1.9	37

**SCHEME 1.** Acid-catalyzed Mechanism for 1,4-Butanediol Dehydration with H<sup>+</sup> Serving as the Catalyst<sup>4</sup>



hydronium ion. The resulting oxonium ion undergoes a rate-limiting intramolecular nucleophilic substitution to liberate H<sub>2</sub>O and form a protonated THF intermediate. The protonated ether then quickly deprotonates to yield the product THF. This

mechanism has also been advanced for this reaction in strong acid solutions at lower temperatures.<sup>4,33</sup> Taking the second step to be rate determining and the other two to be in quasi-equilibrium, as suggested by Hudson and Barker,<sup>4</sup> leads to the following rate law for the disappearance of BD via H<sup>+</sup> catalysis:

$$-r_{\text{BD}} = k_1[\text{H}^+][\text{BD}] - k_{-1}[\text{H}^+][\text{THF}] \quad (9)$$

where  $-r_{\text{BD}}$  is the rate of disappearance of BD, and  $k_1$  and  $k_{-1}$  are the observable second-order forward and reverse rate constants, respectively, for the reaction. In this analysis, we will consider only the forward reaction for BD dehydration, given by

$$r_{\text{BD} \rightarrow \text{THF}} = k_1[\text{H}^+][\text{BD}] = k_{\text{F}}[\text{BD}] \quad (10)$$

The pseudo-first-order rate constant  $k_{\text{F}}$  ( $k_{\text{F}} = k_1[\text{H}^+]$ ) should be directly proportional to the concentration of H<sup>+</sup> ions, for the mechanism shown in Scheme 1.

To quantitatively assess the effect of added CO<sub>2</sub> on the rate of dehydration, we define a rate increase factor (RIF) as the ratio of  $k_{\text{F}}$  in the presence of CO<sub>2</sub> to that without added CO<sub>2</sub>.

For the mechanism in Scheme 1, the expected increase in rate with added CO<sub>2</sub> can be estimated as the ratio of [H<sup>+</sup>] in HTW with added CO<sub>2</sub> to that in pure HTW. The pH of neutral HTW is 5.7 at 250 °C and 5.9 at 300 °C.<sup>34</sup> For the CO<sub>2</sub>-added experiments, we estimated the pH to be 3.9 and 4.3 at the same temperatures. On the basis of these pH values and the mechanism in Scheme 1, one expects the rate to increase by factors of 60 and 37 for the CO<sub>2</sub>-added experiments at 250 °C and 300 °C, respectively. The experimentally determined RIFs were only 2.9 and 1.9 though, as summarized in Table 2. Thus, the addition of CO<sub>2</sub> was far less effective than predicted by eq 10. These results imply that the reaction is not first order in [H<sup>+</sup>] at these temperatures, but rather exhibits an apparent reaction order less than one. These results further imply that that Scheme 1 does not accurately describe the reaction in HTW at near-neutral conditions.

**Effect of pH.** To resolve the disagreement between the low H<sup>+</sup> reaction order implied by the added-CO<sub>2</sub> experiments and the mechanism-based order of unity expected from the literature, we examined the effect of pH on the pseudo-first-order rate constant for BD dehydration. We conducted BD dehydration experiments in HTW using tubing bomb reactors with either added HCl or NaOH at 200, 250, and 300 °C, and over a pH range of 2.1 to 10.0. Table 3 summarizes these experimental conditions and the results. Only BD and THF were observed as reaction products, and their sum accounted for 94 ± 2% of the moles of BD loaded into the reactors for all tubing bomb experiments.

For these experiments with added acid or base, we calculated the pseudo-first-order rate constant  $k_{\text{F}}$  as

$$k_{\text{F}} = -\frac{1}{t} \ln(1 - X) \quad (11)$$

where  $X$  is the conversion of BD and  $t$  is the batch holding time. Equation 11 is exact for an irreversible first-order reaction, and it provides a reasonable estimate for a reversible first-order reaction far from equilibrium. For example, using eq 11 to

(33) Wisniewski, A.; Szafranek, J.; Sokolowski, J. *Carbohydr. Res.* **1981**, *97*, 229–234.

(34) Marshall, W. L.; Franck, E. U. *J. Phys. Chem. Ref. Data* **1981**, *10*, 295–304.

**TABLE 3.** Summary of Experiments with Added HCl and NaOH

$T$ (°C)	pH	$t$ (min)	$X$	$\log(k_F/s^{-1})$
200	2.1	1060	$0.57 \pm 0.43$	$-5.0 \pm 0.7$
	3.8	1060	$0.16 \pm 0.10$	$-5.6 \pm 0.3$
	7.1	7260	$0.15 \pm 0.10$	$-6.5 \pm 0.3$
250	3.2	15	$0.53 \pm 0.11$	$-3.1 \pm 0.1$
	3.6	20	$0.30 \pm 0.02$	$-3.53 \pm 0.03$
	4.0	180	$0.49 \pm 0.05$	$-4.2 \pm 0.1$
	7.4	180	$0.14 \pm 0.06$	$-4.9 \pm 0.1$
	8.1	990	$0.10 \pm 0.06$	$-5.8 \pm 0.6$
300	4.3	15	$0.33 \pm 0.04$	$-3.4 \pm 0.1$
	4.9	20	$0.51 \pm 0.05$	$-3.2 \pm 0.1$
	8.0	25	$0.07 \pm 0.11$	$-4.4 \pm 0.7$
	10.0	180	$0.019 \pm 0.004^a$	$-5.8 \pm 0.1$

<sup>a</sup> THF yield used as estimate of conversion.

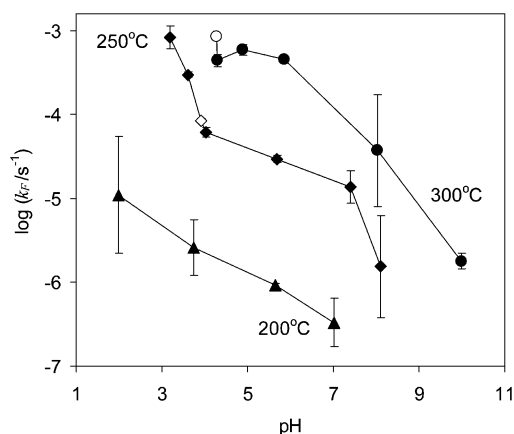


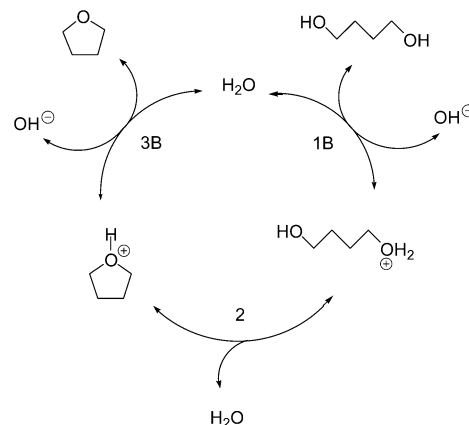
**FIGURE 7.** Effect of pH on pseudo-first-order rate constant for BD dehydration in HTW at 200, 250, and 300 °C. Added- $\text{CO}_2$  rate constants are indicated as open symbols.

estimate  $k_F$  for a reversible reaction with equilibrium yield of 90% from an experiment with 50% conversion overestimates  $k_F$  and  $\log k_F$  by only 5% and 1%, respectively. Over the temperature range of 200–300 °C, the equilibrium conversion for BD dehydration varies from 84% to 92%. In these added-acid and added-base experiments, the conversion ranged from 2 to 57% and was typically less than 40%. Thus, eq 11 provides a reliable estimate for  $\log k_F$  in these experiments.

Figure 7 illustrates the effect of pH on  $k_F$  at 200, 250, and 300 °C. Over large changes in pH,  $\log k_F$  generally increases with increasing acidity. Over smaller changes in pH, however, the effect of added acid or base appears to vary depending on pH regime. For example, at 250 °C, the rate constant displays a strong dependence on pH at  $\text{pH} < 4$  and at  $\text{pH} > 7$ . At near-neutral pH ( $4 < \text{pH} < 7$ ), however, the rate constant is less strongly affected by added acid or base.

The behavior displayed by  $k_F$  in Figure 7 is not consistent with the reaction being first order in  $\text{H}^+$ , as required by the mechanism in the literature. Rather, the apparent reaction orders for  $\text{H}^+$  are 0.30, 0.44, and 0.44 at 200, 250, and 300 °C, respectively. Moreover, Figure 7 shows that  $\log k_F$  is not a linear function of pH, but rather depends on pH in a more complicated manner.

To assess the consistency between the added  $\text{CO}_2$  and added HCl experiments, which were done in two different types of batch reactors and had rate constants determined two different ways, we included the  $k_F$  values from Table 2 in Figure 7. These values show that the rate of dehydration observed with added

**SCHEME 2.** Acid-catalyzed Mechanism for 1,4-Butanediol Dehydration with Water Serving as the Catalyst

$\text{CO}_2$  is consistent with the rates observed with added mineral acid at similar pH. This agreement supports the notion that the increases in rate observed with added  $\text{CO}_2$  were due to lower values of pH in those experiments, which resulted from the formation and dissociation of carbonic acid. This agreement further shows that the treatment of the kinetics data from the autoclave and the tubing bombs led to consistent results.

**Mechanism.** To explain the effect of pH on  $\log k_F$ , we examined the mechanism of BD dehydration. Scheme 1 displays the classical acid-catalyzed reaction, wherein the catalytic action is initiated by the transfer of a proton from a hydronium ion to the reactant. However, in an aqueous medium, it is possible that water may also serve as a proton donor. Participation by water was previously suggested<sup>27</sup> but without any mechanistic details. We propose that water can act as the proton source to catalyze the dehydration of BD, as shown in Scheme 2. This mechanism proceeds through the same organic intermediates as Scheme 1.

We use Schemes 1 and 2, together, to describe the pH dependence of the reaction in HTW. Both  $\text{H}^+$  and  $\text{H}_2\text{O}$  serve as proton-donating acid catalysts. Taking step 2 to be rate determining and steps 1A, 1B, 3A, and 3B to be in quasi-equilibrium leads to the pseudo-first-order rate equation below.

$$-r_{\text{BD}} = k_F[\text{BD}] - k_R[\text{THF}] \quad (12)$$

where

$$k_F = k_2 \frac{k_{1A}[\text{H}^+] + k_{1B}[\text{H}_2\text{O}]}{k_{-1A} + k_{-1B}[\text{OH}^-]} = k_2 K_F \quad (13)$$

and

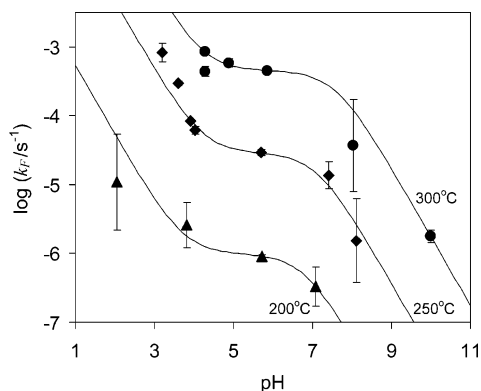
$$k_R = k_{-2} \frac{k_{-3A}[\text{H}^+] + k_{-3B}[\text{H}_2\text{O}]}{k_{3A} + k_{3B}[\text{OH}^-]} = k_{-2} K_R \quad (14)$$

Positive and negative numerical coefficients of the rate constant subscripts in eqs 13 and 14 indicate reaction in the clockwise and counterclockwise directions, respectively, in Schemes 1 and 2.  $K_F$  and  $K_R$  represent quantities akin to equilibrium constants for the quasi-equilibrated protonation of BD and THF, respectively, and are herein referred to as apparent equilibrium constants.

**TABLE 4.** Estimates for the Parameters in Equation 15<sup>a</sup>

<i>T</i> (°C)	log <i>k<sub>A</sub></i>	log <i>k<sub>B</sub></i>	log <i>k<sub>C</sub></i>
200	-2.3 ± 0.5	-6.01 ± 0.02	-6.8 ± 0.2
250	-0.33 ± 0.06	-4.54 ± 0.06	-7.1 ± 0.4
300	0.87 ± 0.07	-3.34 ± 0.05	-7.6 ± 0.2

<sup>a</sup> Uncertainties represent one standard deviation. Units of *k<sub>A</sub>*, *k<sub>B</sub>*, and *k<sub>C</sub>* are L mol<sup>-1</sup> s<sup>-1</sup>, s<sup>-1</sup>, and mol L<sup>-1</sup>, respectively.

**FIGURE 8.** Agreement between eq 15 and log *k<sub>F</sub>* vs pH data at 200–300 °C.

Equation 13, an expression for *k<sub>F</sub>* based on the mechanisms presented in Schemes 1 and 2, can be written as a three-parameter equation that can be used to fit log *k<sub>F</sub>* versus pH data:

$$k_F = \frac{k_A[\text{H}^+] + k_B}{1 + \frac{k_C}{[\text{H}^+]}} \quad (15)$$

where

$$k_A = k_2 \frac{k_{1A}}{k_{-1A}} \quad (16)$$

$$k_B = k_2 \frac{k_{1B}}{k_{-1A}} [\text{H}_2\text{O}] \quad (17)$$

and

$$k_C = K_w \frac{k_{-1B}}{k_{-1A}} \quad (18)$$

We fit eq 15 to the log *k<sub>F</sub>* versus pH data at 200–300 °C, including data from the added-CO<sub>2</sub> experiments, using Scientist. We performed a weighted, nonlinear-least-squares fit, using the reciprocal of the variance of each point as the statistical weight. Table 4 provides the resulting estimates for *k<sub>A</sub>*, *k<sub>B</sub>*, and *k<sub>C</sub>* at each temperature. Figure 8 shows that eq 15 provides a good description of the experimental data over the entire range of pH and temperature. Additionally, Figure 8 shows that the reaction exhibits general acid catalysis at near-neutral pH, and specific acid catalysis at high and low pH.

The ability of eq 15 to capture the trends in the data at each temperature suggests that water, in addition to the hydronium ion, functions as a proton donor in the dehydration of BD in HTW. Similar acid/base behavior has been noted previously

for water in the hydrothermal cleavage of bisphenol A,<sup>35</sup> where water, rather than the native hydroxyl ion, serves as a proton acceptor at near-neutral pH. The kinetic significance of the water-catalyzed path for BD dehydration in HTW can be appreciated by comparing the rate constant *k<sub>F</sub>* observed at neutral pH (Table 1) with the value of the H<sup>+</sup>-catalyzed rate constant calculated at neutral pH, which is given by *k<sub>A</sub>*[H<sup>+</sup>] and is the hypothetical rate constant that would be observed if H<sub>2</sub>O did not behave as a proton donor in the reaction. The observed rate constant, *k<sub>F</sub>*, is 30–90 times greater than the hypothetical H<sup>+</sup>-catalyzed rate constant over this temperature range. This result suggests that the dehydration of BD in HTW without catalyst would be 1 to 2 orders of magnitude slower, if not for the ability of H<sub>2</sub>O to transfer a proton directly to BD.

The pH dependence of the dehydration reaction in HTW can be discussed in terms of H<sup>+</sup> catalysis (reactions 1A and -1A in Scheme 1) and H<sub>2</sub>O catalysis (reactions 1B and -1B in Scheme 2) and can be described based on eq 13 as follows. Under strongly acidic conditions, both the protonation and deprotonation of BD are dominated by H<sup>+</sup> catalysis (*k<sub>1A</sub>*[H<sup>+</sup>] ≫ *k<sub>1B</sub>*[H<sub>2</sub>O] and *k<sub>-1A</sub>* ≫ *k<sub>-1B</sub>*[OH<sup>-</sup>]). In this scenario, eq 13 simplifies to *k<sub>F</sub>* = *k<sub>2</sub>**K<sub>1A</sub>*[H<sup>+</sup>] = *k<sub>A</sub>*[H<sup>+</sup>]. As the pH increases, the protonation of BD by H<sub>2</sub>O becomes increasingly significant compared to protonation by H<sup>+</sup>. At near-neutral pH, the protonation is dominated by H<sub>2</sub>O catalysis (*k<sub>1B</sub>*[H<sub>2</sub>O] ≫ *k<sub>1A</sub>*[H<sup>+</sup>]). The deprotonation, however, still occurs primarily via the H<sup>+</sup>-catalyzed path (*k<sub>-1A</sub>* ≫ *k<sub>-1B</sub>*[OH<sup>-</sup>]). Under these conditions, eq 13 simplifies to *k<sub>F</sub>* = (*k<sub>2</sub>**k<sub>1B</sub>*/*k<sub>-1A</sub>*)[H<sub>2</sub>O] = *k<sub>B</sub>*. As the pH increases further, deprotonation to BD via H<sub>2</sub>O catalysis becomes faster than that via H<sup>+</sup> catalysis (*k<sub>-1B</sub>*[OH<sup>-</sup>] ≫ *k<sub>-1A</sub>*), because of the increase in OH<sup>-</sup> concentration. Thus, under strongly basic conditions, H<sub>2</sub>O catalysis dominates the reaction, (*k<sub>1B</sub>*[H<sub>2</sub>O] ≫ *k<sub>1A</sub>*[H<sup>+</sup>] and *k<sub>-1B</sub>*[OH<sup>-</sup>] ≫ *k<sub>-1A</sub>*), and eq 13 can be simplified to *k<sub>F</sub>* = (*k<sub>2</sub>**K<sub>1B</sub>*/*K<sub>w</sub>*)[H<sub>2</sub>O][H<sup>+</sup>] = *k<sub>B</sub>*[H<sup>+</sup>]/*k<sub>C</sub>*. This analysis suggests that the effect of pH on the dehydration reaction is to alter the form of the apparent equilibrium constant *K<sub>F</sub>*, rather than to promote fundamentally different reaction mechanisms<sup>36,37</sup> or changes in rate determining step,<sup>38</sup> as observed in other systems. Table 5 summarizes the effect of pH on the apparent equilibrium constant and dehydration reaction.

**Implications for CO<sub>2</sub> Addition.** The addition of CO<sub>2</sub> to HTW may be an environmentally benign method of achieving increased rates of acid-catalyzed reactions, and may therefore be a technique for making HTW more industrially competitive as a reaction medium. The curves in Figure 8 suggest that, for BD dehydration in HTW, the addition of sufficient quantities of CO<sub>2</sub> to the reaction medium will lead to increased rates of reaction. Quantitatively, however, these data suggest that significant increases in the reaction rate will only be achieved with added CO<sub>2</sub> when the addition of CO<sub>2</sub> yields a pH that is at least 2 to 3 units lower than the neutral pH. Hence, at moderate CO<sub>2</sub> loadings (*P*<sub>CO<sub>2</sub></sub> < 100 bar), CO<sub>2</sub> addition may be ineffective for achieving significant rate increases for BD dehydration in HTW. High pressures (100 < *P*<sub>CO<sub>2</sub></sub> < 1000 bar)<sup>39</sup>

(35) Hunter, S. E.; Savage, P. E. *J. Org. Chem.* **2004**, *69*, 4724–4731.

(36) Buurma, N. J.; Blandamer, M. J.; Engberts, J. B. F. *N. J. Phys. Org. Chem.* **2003**, *16*, 438–449.

(37) Salvestrini, S.; Di Cerbo, P.; Capasso, S. *J. Chem. Soc., Perkin Trans. 2* **2002**, 1889–1893.

(38) Fett, R.; Simionatto, E. L.; Yunes, R. A. *J. Phys. Org. Chem.* **1990**, *3*, 620–626.

(39) Hunter, S. E. Ph.D. Thesis, The University of Michigan, Ann Arbor, MI, 2005.

TABLE 5. Summary of Effect of pH on 1,4-Butanediol Dehydration in HTW

pH	dominant BD protonation step	dominant BDH <sup>+</sup> deprotonation step	apparent equilibrium constant expression	simplified $k_F$	H <sup>+</sup> reaction order
low	1A	-1A	$K_F = \frac{k_{1A}[\text{H}^+]}{k_{-1A}}$	$k_F = k_A[\text{H}^+]$	1st
intermed	1B	-1A	$K_F = \frac{k_{1B}[\text{H}_2\text{O}]}{k_{-1A}}$	$k_F = k_B$	0th
high	1B	-1B	$K_F = \frac{k_{1B}[\text{H}_2\text{O}]}{k_{-1B}[\text{OH}^-]}$	$k_F = \frac{k_B}{k_C}[\text{H}^+]$	1st

are required to achieve the low pH conditions where the reaction rate will be significantly greater than the neutral reaction rate. These high-pressure conditions may render CO<sub>2</sub> addition an impractical method of achieving accelerated rates of BD dehydration in HTW.

**Comparison with the Literature.** Nagai et al. proposed eq 19 for BD dehydration based on their  $k_F$  versus [H<sup>+</sup>] data,

$$k_F = k_{\text{acid}}[\text{H}^+] + k_{\text{water}} \quad (19)$$

where  $k_{\text{acid}}$  is the H<sup>+</sup>-catalyzed rate constant and  $k_{\text{water}}$  is the “water-induced” rate constant.<sup>27</sup> Empirical eq 19 can be recovered from mechanism-based eq 15 as a limiting case. When reaction at high pH is neglected ( $k_{-1B}[\text{OH}^-] \ll k_{-1A}$ ), then  $k_F = k_A(\text{H}^+) + k_B$ .

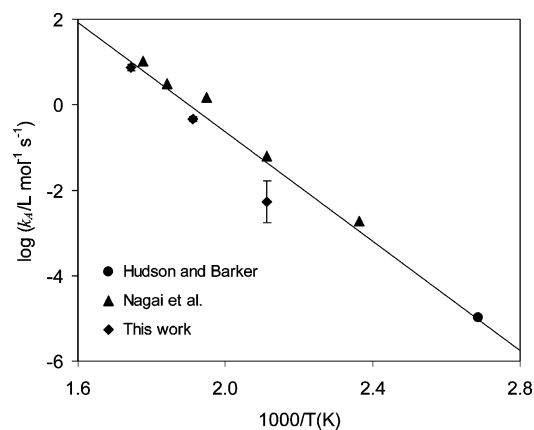
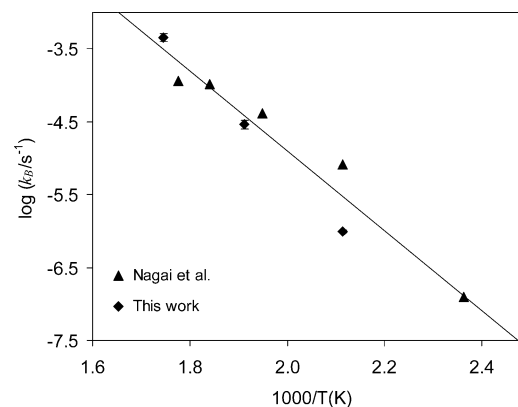
Equation 19 implies that a linear relationship should exist between  $k_F$  and the H<sup>+</sup> concentration. The data in Figure 8 and eq 15 demonstrate that  $k_F$  is only a linear function of [H<sup>+</sup>] for the limiting case of intermediate and acidic pH, the region explored by Nagai et al. Over the larger range of pH examined here,  $k_F$  depends on [H<sup>+</sup>] in a more complicated manner. When considering acid/base-catalyzed reactions, where the H<sup>+</sup> and OH<sup>-</sup> concentrations and observed rate constant can vary by several orders of magnitude, it is advantageous to examine  $k_F$  versus [H<sup>+</sup>] data on a logarithmic scale.<sup>40</sup> Significant information regarding acid/base-catalyzed reactions in HTW can be obtained by examining the observed rate constant over a wide range of pH, including acidic-, basic-, and neutral-pH conditions.

We compared the data obtained for  $k_A$  and  $k_B$  in this investigation with that of Nagai et al.<sup>27</sup> and Hudson and Barker.<sup>4</sup> Nagai et al. provide  $k_A$  and  $k_B$  in HTW at 150–290 °C, whereas Hudson and Barker provide  $k_A$  at 99 °C. Figure 9 shows good consistency among the  $k_A$  data from 99 to 300 °C. Additionally, Figure 10 demonstrates consistency between the  $k_B$  data of Nagai et al. and that of the present work, over a temperature range of 150–300 °C. Figure 11 demonstrates an inverse relationship of  $k_C$  with temperature, which is permissible for such a lumped, or composite, rate constant. We performed linear regression (ln  $k$  vs 1/ $T$ ) of the data in Figures 9–11 to obtain the apparent activation energy and preexponential factor of each lumped rate constant. Table 6 displays the estimated values.

Having obtained Arrhenius parameters for the rate constants in eq 15, we next used the mechanism-based model to examine the behavior of BD dehydration as a function of pH over a wide range of temperature. Figure 12 shows  $k_F$  over the pH range of

1–11 and a temperature range of 50–350 °C, calculated using eq 15 and the parameters in Table 6.

At each temperature, the intermediate pH regime, as defined in Table 5, can be estimated as having lower and upper bounds of [H<sup>+</sup>] =  $k_B/k_A$  and [H<sup>+</sup>] =  $k_C$ , respectively. These bounds are plotted in Figure 12. As shown in the figure, this intermediate regime expands and shifts to higher pH with increasing temperature. Additionally, Figure 12 shows the neutral pH of H<sub>2</sub>O at each temperature. At low temperature, the neutral pH is greater than the upper bound of the intermediate regime. As temperature increases and  $K_W$  approaches its maximum, the neutral pH moves within the intermediate regime. The location of the intermediate region with respect to the neutral pH is

FIGURE 9. Temperature dependence of  $k_A$ .FIGURE 10. Temperature dependence of  $k_B$ .

(40) Gates, B. C. *Catalytic Chemistry*; John Wiley & Sons: New York, 1992.

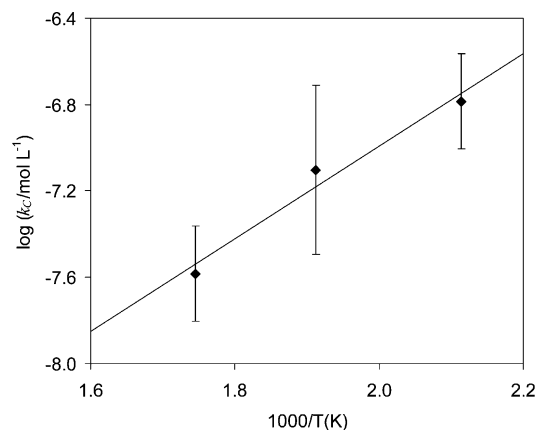


FIGURE 11. Temperature dependence of  $k_C$ .

TABLE 6. Arrhenius Parameters for  $k_A$ ,  $k_B$ , and  $k_C^a$

rate constant	log A	$E_A$ (kcal mol <sup>-1</sup> )
$k_A$	12.2 ± 2.4	29.3 ± 5.4
$k_B$	6.1 ± 2.8	25.1 ± 6.4
$k_C$	-11.3 ± 9.2	-9.8 ± 21.7

<sup>a</sup> Units of  $k_A$ ,  $k_B$ , and  $k_C$  are L mol<sup>-1</sup> s<sup>-1</sup>, s<sup>-1</sup>, and mol L<sup>-1</sup>, respectively.

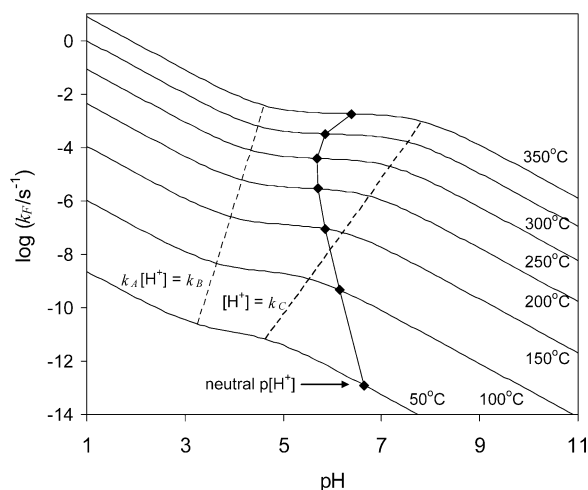


FIGURE 12. Effect of pH and temperature for BD dehydration in H<sub>2</sub>O at elevated temperatures. The intermediate pH range, as defined in Table 5, is located at each temperature between the two dashed lines. Each dashed line represents the pH around which the reaction transitions from 1st to 0th order in H<sup>+</sup>.

significant when attempting to use pH to tune the reaction to achieve higher rates. At lower temperatures, the low pH regime, as defined in Table 5, begins at lower pH, and is further away from neutral pH. At higher temperatures, the low pH regime begins at higher pH, and is generally closer to the neutral pH. Hence, the effect of decreasing pH (e.g., adding acid) on the rate will be a function of temperature and for BD dehydration in H<sub>2</sub>O will generally increase with increasing temperature.

## Conclusions

1,4-Butanediol dehydrates reversibly in HTW at 200–350 °C to selectively yield tetrahydrofuran. No added catalyst is required for the reaction, although addition of mineral acid or

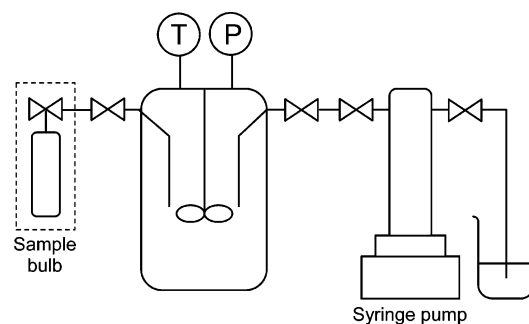


FIGURE 13. Schematic representation of autoclave batch reactor used for neutral HTW and CO<sub>2</sub>-added BD dehydration experiments.

CO<sub>2</sub> will accelerate the rate. The reaction follows pseudo-first-order kinetics in reactant and product, and equilibrium THF yields are greater than 90% at temperatures above 250 °C. The dehydration reaction is endothermic, exhibiting a heat of reaction of 1.0 kcal/mol.

The use of HTW for the synthesis of THF via 1,4-butanediol dehydration has potential advantages over commercial synthesis in strong acid solutions or over solid acid catalysts. In HTW, no catalyst is necessary for the reaction, and dehydration rates exceed those at lower temperature in the presence of strong mineral acid catalyst. The equilibrium yield of THF (>90%) is comparable with that typically achieved in the Reppe and propylene oxide processes (95%). Hence, THF synthesis in HTW may be a green and practical alternative to conventional catalytic processes.

The dehydration of 1,4-butanediol occurs with a pH-independent rate at near-neutral pH in HTW. In contrast, the dehydration is first-order in H<sup>+</sup> concentration at strongly acidic or strongly basic pH. This behavior is consistent with an acid-catalyzed dehydration mechanism, where not only H<sup>+</sup>, but also H<sub>2</sub>O, serve as proton donors. At low and high pH, H<sup>+</sup> and H<sub>2</sub>O serve as the primary catalysts, respectively. However, at near-neutral pH, butanediol is protonated via reaction with H<sub>2</sub>O (water catalysis), and deprotonation of the protonated butanediol produces H<sup>+</sup> (H<sup>+</sup> catalysis). Hence, the elevated values of  $K_w$  for water at high temperatures, and the associated H<sup>+</sup> concentrations, are not primarily responsible for the occurrence of BD dehydration in HTW in the absence of added catalyst. Rather, water itself plays the more important role as a proton donor. This work thus highlights the importance of verifying the role of  $K_w$  in acid- and base-catalyzed reactions in neutral HTW through experimentation with added acid and base over a wide range of pH.

## Experimental Section

**Materials.** Deionized water was obtained from an in-house water purification system, which contained water softener (ion exchange), reverse osmosis, high-capacity ion exchange, UV sterilization, ultrapure ion exchange, and submicron filtration units. BD, THF, 0.2 M HCl, and 0.5 M NaOH were obtained from a commercial supplier. All chemicals were used as received.

**Reactors.** We conducted THF synthesis experiments in the two different batch reactor systems described in detail below.

**1. Autoclave Reactor.** To obtain yield versus time profiles in HTW and in HTW with added CO<sub>2</sub>, we employed a 440 mL hastelloy batch reactor from a commercial supplier. Figure 13 depicts the autoclave apparatus. In this system, deionized water was first loaded into the reactor body, and the reactor was sealed. The quantity of water loaded was determined such that the expanded

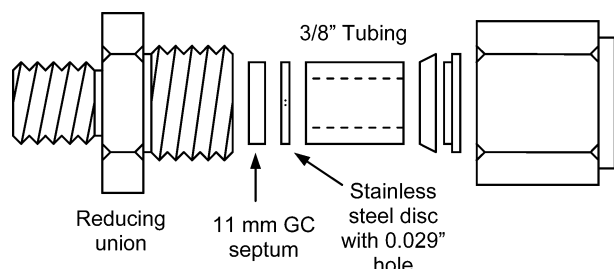


**FIGURE 14.** Exploded-view illustration of septum-containing attachment utilized during autoclave sample recovery.

water volume at reaction temperature occupied roughly 95% of the reactor volume, based on the saturation density of pure liquid water.<sup>29</sup> To degas the water, the reactor headspace was filled with roughly 69 bar of  $N_2$ , agitated for 15 min at roughly 800 rpm with an internal stirrer, and then depressurized. This process was repeated at least two additional times.

When required,  $CO_2$  was next loaded into the reactor headspace through a port in the top of the reactor head. The initial (nonequilibrium) partial pressure of  $CO_2$  in the reactor just after loading was roughly 55 bar, and it decreased with time before heating, as the gas dissolved in the water. To promote dissolution of the  $CO_2$  in the water, the reactor agitator was set to roughly 1000 rpm during the reactor heating process. The heat-up time was always greater than 1 h, which provided adequate time<sup>41</sup> to reach  $CO_2$ – $H_2O$  vapor–liquid equilibrium prior to initiating the reaction.

The reactor was next heated to the desired reaction temperature, which was stable to within 3 °C of the set point in all experiments and typically did not vary by more than 2 °C during a reaction. To initiate the reaction, roughly 10 mL of BD were loaded into the hot, pressurized reactor through a dip tube extending into the reactor body using a syringe pump set to operate in constant pressure mode at 34–69 bar greater than the reactor pressure. The end of this loading procedure, which took 5–10 s, was regarded as the initial time ( $t = 0$ ) for the reaction. The reaction mixture was agitated throughout the reaction at roughly 1000 rpm.

Liquid phase samples were removed from the reactor periodically through a dip tube and collected in stainless steel sample bulbs that had an internal volume of roughly 0.9 mL. To ensure that the sample acquired was representative of the reactor contents at the time at which it was taken, at least one presample was taken just prior to the desired sample time to purge the sampling line of any residual material. All sample bulbs were cooled in a refrigerator for at least 30 min before opening to maximize product recovery.

To recover the reactor samples for analysis, sample bulbs were first depressurized using a septum-containing attachment, represented in Figure 14. The device was attached to the sample bulb, and the bulb contents were allowed to expand into a 5 or 10 mL syringe, containing roughly 1 mL of acetone, inserted through the septum in the attachment. This process was repeated until the bulb was no longer pressurized. The bulb was then inverted, and opened. Remaining bulb contents were rinsed with acetone. All acetone rinses, including the solutions obtained during depressurization, were collected in a 10 mL flask. After recovery, the flasks were filled to the 10 mL line with solvent, and samples were removed from the flask and placed in vials for analysis. The molar yield  $Y_i$  of species  $i$  was calculated as  $Y_i = C_i/C_T$ , where  $C_i$  is the molar concentration of species  $i$  and  $C_T$  is the total concentration of organic species in the reactor. This quantity was taken to be equal to  $C_{BD} + C_{THF}$  since the reactant and product were the only species detected throughout the reaction.

We calculated the 95% confidence interval for the yield of THF using four samples that were obtained at 350 °C after the reaction had reached equilibrium. Because these samples were taken after

reaching equilibrium, they can be viewed as multiple samples at the same conditions. The average  $Y_{THF}$  was equal to 0.929 with a 95% confidence interval of 0.003. According to this analysis, then, the uncertainty for molar yields obtained from the autoclave reactor can be estimated as less than 0.01 at the 95% confidence level.

The measured value of  $C_T$  at short times was 95 to 99% of the initial BD concentration  $C_{BD,0}$ , which was calculated as the number of moles of BD loaded divided by the mass of  $H_2O$  loaded. This result indicates that nearly all of the BD resided initially in the liquid phase. Additionally,  $C_T$  was time invariant at 200 and 250 °C, but it decreased by roughly 15% at 300 °C and roughly 30% at 350 °C over the course of the reaction. This decrease in  $C_T$  is not due to the formation of additional reaction products. We observed no other product peaks in the chromatograms, and no previous investigator<sup>26,27</sup> reported the formation of species other than BD or THF at temperatures up to 350 °C. Rather, the decrease in  $C_T$  at the higher temperatures is likely due to the transfer of organic species, especially the more volatile THF, from the liquid phase to the vapor phase during the experiment. The larger change in  $C_T$  at higher temperatures is a reflection of the higher specific volume of  $H_2O$  at those conditions, a larger number of samples and sample line rinses being taken during those reactions, and more THF being present. Because the reaction is first order in BD and THF concentration, though, and because the decrease in  $C_T$  was minimal during acquisition of the first 6–8 samples, we do not expect these decreases in  $C_T$  to affect the observed reaction kinetics. This expectation was verified by the kinetics determined in tubing bomb reactors, which did not suffer from this sampling-induced potential problem and yielded results consistent with those determined from autoclave experiments.

**2. Tubing Bomb Reactors.** For experiments with added acid and added base, and for preliminary THF synthesis experiments, we used 0.6 mL tubing bomb reactors. Detailed information concerning the reactor assembly, reaction procedure, and product recovery appeared in a previous paper.<sup>42</sup> Roughly 15 mg of BD was carefully measured and then loaded into each tubing bomb reactor. The required amounts (3–180  $\mu$ L) of HCl or NaOH solutions were added after loading degassed water. Tubing bomb reactors that had been used for HTW experiments with added acid or base exhibited residual catalytic effects when later used to perform experiments without added catalyst. Hence, once a set of reactors had been exposed to strong acid, that set was exclusively used for experiments with added strong acid, and likewise for those reactors with added base. Uncertainty for results obtained using these tubing bomb reactors was determined as the 95% confidence interval, on the basis of at least three independent experiments conducted under identical conditions.

**Product Analysis.** We used a gas chromatograph, equipped with a flame ionization detector, autosampler, and 50 m  $\times$  0.2 mm  $\times$  0.33  $\mu$ m HP-5 capillary column, for product analysis. The temperature program comprised a 9 min soak at 70 °C, followed by a 70 °C/min ramp to 240 °C, which was held for 9 min. Products were identified by matching retention times with those of known standards and quantified using calibration curves, which were calculated from the chromatographic results of four to six standards.

**Calculation of pH.** The pH of neutral HTW and HTW with added acid or base was calculated using literature values for  $K_w$ <sup>34</sup> and recognizing that HCl<sup>43</sup> and NaOH<sup>44</sup> are essentially completely dissociated in HTW. To estimate the pH in the added- $CO_2$  experiments, we applied the development of Hunter and Savage,<sup>25</sup> wherein the reactor contents are modeled as a two-phase, two-component mixture with vapor–liquid equilibrium between  $H_2O$  and  $CO_2$ . Recognizing that the second dissociation of carbonic acid,

(42) Hunter, S. E.; Felczak, C. A.; Savage, P. E. *Green Chem.* **2004**, *6*, 222–226.

(43) Frantz, J. D.; Marshall, W. L. *Am. J. Sci.* **1984**, *284*, 651–667.

(44) Chen, X. M.; Gillespie, S. E.; Oscarson, J. L.; Izatt, R. M. *J. Solution Chem.* **1992**, *21*, 803–824.

(41) Takenouchi, S.; Kennedy, G. C. *Am. J. Sci.* **1964**, *262*, 1055–1074.

vapor- and liquid-phase nonidealities, and the influence of the small amount of dissolved CO<sub>2</sub> on the aqueous-phase density are negligible,<sup>39</sup> one can estimate the molal H<sup>+</sup> concentration according to

$$(\text{H}^+) = \frac{K_{\text{W}}}{(\text{H}^+)} + \left( \frac{K_{\text{a1}}}{(\text{H}^+)} \right) \frac{C_{\text{CO}_2}^{\text{T}}}{\rho_{\text{H}_2\text{O}} f + \frac{1-f}{\frac{(\text{H}_2\text{O})}{H} - RT}} \quad (20)$$

where  $K_{\text{a1}}$  is the first dissociation constant of carbonic acid,<sup>45</sup>  $\rho_{\text{H}_2\text{O}}$  is the density of saturated liquid water,<sup>29</sup>  $H$  is the Henry's constant for CO<sub>2</sub>,<sup>46</sup>  $C_{\text{CO}_2}^{\text{T}}$  is the total number of moles of CO<sub>2</sub> added to the reactor divided by the reactor volume,  $f$  is the fraction of the reactor volume occupied by the aqueous phase,  $R$  is the gas constant,  $T$  is absolute temperature, and the curved brackets represent molal

(45) Patterson, C. S.; Slocum, G. H.; Busey, R. H.; Mesmer, R. E. *Geochim. Cosmochim. Acta* **1982**, *46*, 1653–1663.

(46) Crovetto, R. *J. Phys. Chem. Ref. Data* **1991**, *20*, 575–589.

concentration. In the autoclave experiments, the value of  $f$  changes as samples are withdrawn. In the experiments presented here, however, the effect of sample withdrawal on pH was less than 0.05 pH units.

In this paper, we express the concentration of H<sup>+</sup> in units of molarity to be consistent with all other concentrations used in the kinetics analysis. Thus our definition of pH herein is as  $-\log [\text{H}^+]$ , rather than the more rigorous definition on the molal scale as  $\text{pH} = -\log (\text{H}^+)$ , where the square and curved brackets represent molar and molal concentrations, respectively. The density of liquid water at high temperatures is less than 1 kg/L, and hence molal and molar concentrations are not numerically equal in HTW as they are in ambient liquid water. The quantities are related as  $\text{pH}_{\text{molar}} = \text{pH}_{\text{molal}} - \log \rho_{\text{H}_2\text{O}}$  (kg/L).

**Acknowledgment.** We thank Brendon Webb for his assistance in conducting tubing bomb reactor experiments. We also acknowledge the financial support from the ACS-PRF (Grant 37603-AC9) and NSF (graduate fellowship to S.E.H. and Grant CTS-0218772).

JO0610170